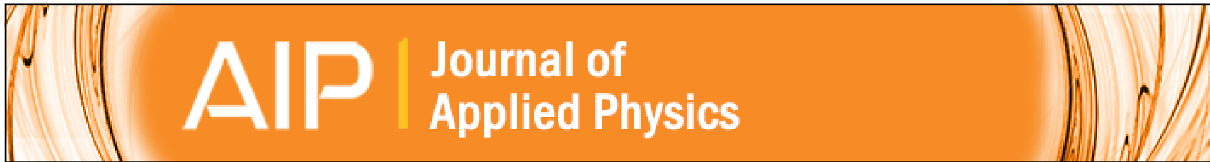


# Thermal stability of the electrical isolation in n-type gallium arsenide layers irradiated with H, He, and B ions

J. P. de Souza, I. Danilov, and H. Boudinov

Citation: Journal of Applied Physics **81**, 650 (1997); doi: 10.1063/1.364229
View online: http://dx.doi.org/10.1063/1.364229
View Table of Contents: http://scitation.aip.org/content/aip/journal/jap/81/2?ver=pdfcov
Published by the AIP Publishing

Re-register for Table of Content Alerts
Create a profile.
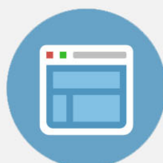
Sign up today!

[This article is copyrighted as indicated in the article. Reuse of AIP content is subject to the terms at: http://scitation.aip.org/termsconditions. Downloaded to ] IP: 200.130.19.173 On: Fri, 21 Mar 2014 18:03:40

# Thermal stability of the electrical isolation in *n*-type gallium arsenide layers irradiated with H, He, and B ions

J. P. de Souza,[a] I. Danilov, and H. Boudinov
*Instituto de Física, UFRGS, 91501-970 Porto Alegre, R.S., Brazil*

(Received 10 April 1996; accepted for publication 9 September 1996)

The stability of the electrical isolation in $n$-type GaAs layers irradiated with ions of different mass is compared. The irradiations were performed with proper doses of $^{1}H^{+}$, $^{4}He^{+}$, or $^{11}B^{+}$ ions to create specific damage concentration level which lead to: (i) the trapping of practically all the carriers ($R_s \approx 10^8$ Ω/□), (ii) the onset of hopping conduction ($R_s \approx 10^8$ Ω/□), and (iii) a significant hopping conduction ($R_s \approx 10^6$ Ω/□). Irrespectively of the ion mass, the temperature range for which the isolation is preserved, i.e., $R_s > 10^8$ Ω/□, extends up to 200 or ≈ 600 °C, respectively, for the cases (i) and (ii). In case (iii), this range comprises temperatures from ≈ 400 to 650 °C. Annealing stages at 200 and 400 °C recover in a great extent the conductivity and improve the carrier mobility in low dose irradiated samples [case (i)]. In samples irradiated to higher doses [cases (ii) and (iii)], the conductivity recovers in a single stage. © *1996 American Institute of Physics.* [S0021-8979(96)04324-1]

## I. INTRODUCTION

Ion implantation is an essential process for the production of modern devices and integrated circuits (ICs) in Si and compound semiconductor technologies. In the case of III-V compound semiconductor, there are two important applications. The first is the implantation of dopants to establish proper $n$- or $p$-type conductivity. The second is the implantation of ions like $H^+$, $He^+$, $B^+$, $O^+$, etc., to convert a doped layer to a highly resistive one. This latter application is called implantation induced isolation or isolation by ion irradiation.[1] In complex GaAs ICs, the backgating effect is of great concern to IC designers because of the associated difficulties imposed to the IC design. This detrimental phenomenon consists in the electrical interaction between neighbor devices resulting in the reduction of the drain-to-source current in field effect transistors by the negative biasing of a closely spaced $n$-type contact.[2] It is known that the ion irradiation of the semi-insulating (SI) regions between neighbor devices greatly minimizes the backgating effect.[3,4]

The irradiation is performed with an ion penetration depth larger than that of doped layer to be isolated. For simplicity and easy control light ions are preferred, since penetration depth up to few microns can be attained with the currently available energies of the industrial implanters. Frequently, the dose is chosen high enough such that conduction via hopping between nearby defects is established.[5] A post-irradiation annealing conducted at typically 300–500 °C is then required to suppress the hopping conduction and increase the $R_s$ from an initial value of $\approx 10^5 - 10^6$ Ω/□ to above $10^8$ Ω/□. The isolation is stable up to the temperature at which most of the irradiation damage anneals out and in the best cases reaches ≈600 °C. Typically, the isolation is the last step in the front-end-of-the-line processing in virtue of its relatively poor thermal stability.

The isolation results from carrier trapping at deep energy levels, associated either to the irradiation damage or specific implanted chemical impurities. In a previous publication,[6] we proposed that antisite defects created by the replacement collisions and/or their related defect complexes constitute the carrier trapping centers.

Although the implantation for isolation is currently used in GaAs ICs[7,8] and discrete device[9,10] technologies a systematic study of the dependence of the thermal stability with the ion mass and ion dose is still missing in the literature. Furthermore, the physical processes involved with the isolation formation and its thermal stability are not yet completely understood.

The thermal stabilities after irradiation with different ion mass were compared in previous publications.[1,11] The published data, regarding sheet resistance after annealing of $H^+$, $B^+$, and $O^+$ irradiated samples, suggest that the thermal stability increases with the increasing of the ion mass. However, uncertainties in the as-irradiated damage concentration after the different mass ion implants certainly preclude that a correlation between the thermal stability and the ion mass could be established.

In the present work, the thermal stability of the electrical isolation of $n$-type layers after irradiations with $^{1}H^{+}$, $^{4}He^{+}$, and $^{11}B^{+}$ is systematically studied. The samples were irradiated to create similar damage concentration using ions of different masses. The results show that the thermal stability of the isolation depends primarily on the irradiation damage concentration. The ion mass has only a marginal importance in the thermal stability behavior.

## II. EXPERIMENT

Semi-insulated liquid-encapsulated crystal (LEC) GaAs wafers of ⟨100⟩ orientation were cleaned with organic solvents and etched to a depth of 4 μm in a solution of $NH_4(OH) : H_2O_2 : H_2O$ (3:1:30 vol.). The wafers were implanted with $^{47}SiF^{+}$ or $^{29}Si^{+}$ to a dose of $5.0 \times 10^{13}$ cm$^{-2}$ at 50 or 30 keV, respectively. The electrical activation of the implanted Si was performed by capless (Si proximity) rapid thermal annealing (RTA) at 850 °C for 10 s. The thickness of

[a]Electronic mail: souz@if.ufrgs.br

 © 1997 American Institute of Physics

[This article is copyrighted as indicated in the article. Reuse of AIP content is subject to the terms at: http://scitation.aip.org/termsconditions. Downloaded to ] IP: 200.130.19.173 On: Fri, 21 Mar 2014 18:03:40

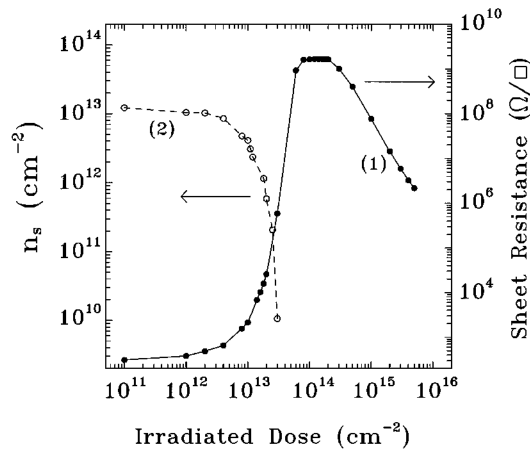


FIG. 1. Sheet resistance $R_s$ [curve (1)] and sheet carrier concentration $n_s$ [curve (2)] in GaAs sample versus $^1H^+$ irradiation dose, at the energy of 50 keV.

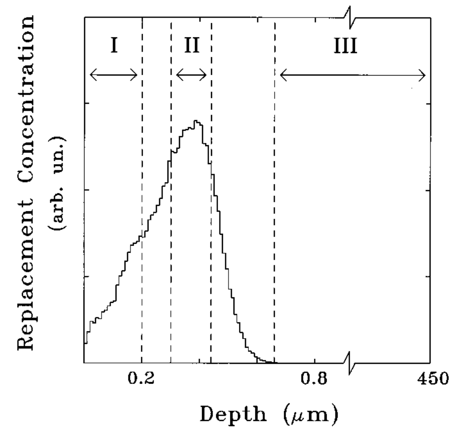


FIG. 2. TRIM code simulated profile of the replacement collision concentration in GaAs irradiated with 50 keV $H^+$. Slab I contains the doped layer, slab II comprises the peak of the damage distribution, and slab III is formed by the underneath SI substrate.

the $n$-doped layer, measured by secondary-ion-mass spectroscopy (SIMS), is 0.2 μm (at $1.0\times10^{16}$ $cm^{-3}$ level). Two types of devices were prepared: resistors of $3\times6$ $mm^2$ rectangular shape and $5\times5$ $mm^2$ Van der Pauw devices.[12] The ohmic contacts to the samples were formed by In applied to the GaAs surface and alloyed at ≈ 200 °C for 2 min. Typical sheet resistances of 330 or 450 Ω/□ were measured respectively in the $^{29}Si^+$ or $^{47}SiF^+$ implanted samples. The effective Hall mobility of the carriers ($\mu$) are in the range of 1800–2000 $cm^2$/V s.

The ion irradiations were performed at nominal room temperature with doses in the range of $1\times10^{11}$ $cm^{-2}$ to $5\times10^{15}$ $cm^{-2}$ of $^1H^+$ at 50 keV, $^4He^+$ at 80 keV, and $^{11}B^+$ at 150 keV. The ion current density was maintained in the range of 0.1–0.3 μA/$cm^2$. The estimated projected ranges[13] are 0.39, 0.39, and 0.35 μm, respectively for $H^+$, $He^+$, and $B^+$ ions. The In contact layers formed mask which prevented the irradiation of the underneath GaAs.

Another set of samples was irradiated before formation of the In contacts. In these samples, the areas reserved for ohmic contact were covered with an aluminum foil during ion irradiation.

All the implantations were performed with the sample surface normal tilted by 7° in respect to the beam incidence direction to minimize ion channeling effect.

The irradiated samples were submitted to thermal annealing steps for 300 s in the temperature range from 100 to 700 °C in Ar atmosphere. From 100 to 500 °C the annealing steps were accumulated in samples which have the In contacts formed prior to the irradiation process. At higher temperatures, the samples were annealed with the irradiated face in close proximity with the Si susceptor. Subsequently, the In contacts were prepared.

The electrical measurements in Van der Pauw devices provided $R_s$, sheet carrier concentration ($n_s$), and effective mobility ($\mu$) values. Electrical measurements in the resistors, using a Keithley 617 electrometer, provided only $R_s$ values.

## III. RESULTS AND DISCUSSION

Curve (1) in Fig. 1 presents the $R_s$ versus the accumulated $H^+$ dose in a resistor. At the beginning of the irradiation (dose $<4\times10^{12}$ $cm^{-2}$), $R_s$ increases slowly with the accumulation of the dose. However, for doses above ≈ $1\times10^{13}$ $cm^{-2}$ a sudden variation of $R_s$ is observed. $R_s$ increases about five orders of magnitude when the $H^+$ dose varied from $1\times10^{13}$ to $4\times10^{13}$ $cm^{-2}$. The increase of $R_s$ occurs in consequence of a progressive removal of the carriers and mobility degradation.

Curve (2) in Fig. 1 presents the $n_s$ values evaluated in irradiated Van der Pauw devices. The original $R_s$ of the Van der Pauw devices is identical to that in the resistor used to obtain curve (1) of Fig. 1. The decreasing of $n_s$ with the accumulation of the irradiation dose is a clear evidence of carrier removal, via capture at the trapping centers. The effective Hall mobility ($\mu$) deteriorates in consequence of the ion irradiation. It varied from an initial value of 1800 to 150 $cm^2$/V s after a dose of $3\times10^{13}$ $cm^{-2}$ has been accumulated. When $R_s$ reaches the $1\times10^9$ Ω/□, practically all carriers were captured by the traps.

It was previously demonstrated that the integrated number of replacement collisions along the depth of the doped layer after irradiation to the dose which convert the conductive layer to a highly resistive one, is of the same order of magnitude of the original sheet carrier concentration.[6]

Further accumulation of the dose does not lead to modification of the $R_s$. A plateau forms in curve (1) with $R_s\approx10^9$ Ω/□. This plateau is succeeded by a decreasing of $R_s$ with the increase of the dose. This damage-related conduction is attributed to carrier transport via hopping between nearby defects.[5] Hall effect measurements in samples irradiated with $H^+$ to the dose of $5\times10^{15}$ $cm^{-2}$ indicate $n$-type conductivity with a very low $\mu$ ($<1$ $cm^2$/V s). In agreement with a previous publication,[5] the data in the descending part of the curve (1) indicate that the increasing of the conductivity is proportional to the third power of the dose.


[This article is copyrighted as indicated in the article. Reuse of AIP content is subject to the terms at: http://scitation.aip.org/termsconditions. Downloaded to ] IP: 200.130.19.173 On: Fri, 21 Mar 2014 18:03:40

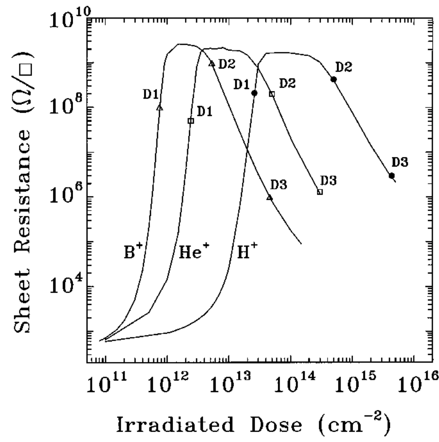


FIG. 3. Sheet resistance versus dose curves for $B^+$ (at 150 keV), $He^+$ (at 80 keV), and $H^+$ (at 50 keV) irradiations in resistors with original $R_s \approx 500$ Ω/□. The points marked in each curve correspond to the doses which create the defect concentration levels to obtain almost complete isolation (D1), the onset of the hopping conduction (D2), or a noticeable hopping conduction (D3).

The energies for the $H^+$, $He^+$, and $B^+$ irradiations were chosen in order to locate the peak of the defect concentration underneath the n-type doped layer. The estimated[13] depth distribution of the replacement collisions for a 50 keV $H^+$ irradiation in GaAs is shown in Fig. 2.

The analysis of the $R_s$ data shown in Fig. 1 [curve (1)] is now developed considering three distinct slabs parallel to the sample surface, as depicted in Fig. 2: slab I, containing the doped layer (thickness of 0.2 $\mu$m); slab II, comprising the peak of the defect distribution; and, slab III, formed by the underneath SI substrate (thickness of 450 $\mu$m). The $R_s$ values shown in curve (1) of Fig. 1 result from the parallel association of three sheet resistances: $R_{s,I}$, of slab I, which original value for the considered sample is 330 Ω/□; $R_{s,II}$, of slab II, originally higher than $10^{12}$ Ω/□, and $R_{s,III}$, the sheet resistance of the underneath SI substrate ($2\times 10^9$ Ω/□). In the low dose region, the parallel association is dominated by the sheet resistance of the doped layer. The increase of the carrier trap concentration in slab I with accumulation of the dose leads to a progressive decreasing of $n_s$ and hence to an increasing of $R_{s,I}$ [see curves (1) and (2) in Fig. 1]. At the threshold dose for isolation,[6] the concentration of the carrier traps present in the doped layer becomes comparable with the original $n_s$. In this situation, $R_{s,I}$ becomes orders of magnitude higher than $R_{s,III}$. Since both $R_{s,I}$ and $R_{s,II}$ are much higher than $R_{s,III}$, the latter sheet resistance dominates the parallel association. Consequently, $R_s \approx R_{s,III}$. This situation persists as long as the defect concentration in slab II is below that required for the onset of hopping conduction. This explains the formation of the plateau in the curve (1) of Fig. 1. The plateau ends when hopping conduction starts in slab II. With further increase of the irradiation dose, the conduction in slab II becomes more significant than in the bulk. In this dose regime, $R_s \approx R_{s,II}$.

In Fig. 3, the $R_s$ versus dose curves are shown for $^1H^+$, $^4He^+$, and $^{11}B^+$ irradiations performed in originally identical resistors. The shift of the curves toward lower doses

TABLE I. The doses of $H^2$, $He^+$, and $B^+$ used to create the specific damage levels D1, D2, and D3.

| | H [$cm^{-2}$] | He [$cm^{-2}$] | B [$cm^{-2}$] |
|---|---|---|---|
| D1 | $2.6\times 10^{13}$ | $2.4\times 10^{12}$ | $7.5\times 10^{11}$ |
| D2 | $5.0\times 10^{14}$ | $5.0\times 10^{13}$ | $5.3\times 10^{12}$ |
| D3 | $4.4\times 10^{15}$ | $3.0\times 10^{14}$ | $4.6\times 10^{13}$ |

scales with the increase of the nuclear energy deposition per income ion in the doped layer.[6]

Considering that the depth distribution of the nuclear energy deposition is almost similar for the used ions it is conceivable to assume that the damage concentrations at equivalent points in the curves of Fig. 3 are approximately similar.

The thermal stability of the isolation was studied using three different damage concentration levels, labelled hereafter as D1, D2, and D3. The marked points in the curves in Fig. 3 correspond to the doses which create the selected damage concentration levels.

After irradiation to create the damage concentration level D1, practically all the carriers are captured by the trapping centers. In the case of D2, a weak hopping conduction is established in the region comprising the peak of the damage profile, where the damage concentration is higher. For both D1 and D2 cases, the $R_s$ values are in the range of $10^8$–$10^9$ Ω/□. After irradiation to create damage concentration D3, a significant hopping conduction is established, resulting in $R_s$ values of $\approx 10^6$ Ω/□.

The doses of $^1H^+$, $^4He^+$, and $^{11}B^+$ required to produce the damage levels D1, D2, and D3 are quoted in Table I.

The evolution of $R_s$ after post-irradiation annealing is shown in Figs. 4(a), 4(b), and 4(c), respectively, in samples irradiated with $^1H^+$, $^4He^+$, and $^{11}B^+$. It is interesting to note that the evolution of $R_s$ with the annealing temperature after irradiation to a similar damage concentration level (D1, D2, or D3) is practically similar, irrespectively of the mass of the used ion.

For D1 case, the stability of the isolation is restricted to temperatures below 200 °C. Above ≈200 °C, a sudden decrease of $R_s$ of 2–3 orders of magnitude is observed. Another annealing stage starting at 400 °C is apparent in the D1 curves.

Some peculiarities of the defect annealing in a sample irradiated to a low dose are disclosed from the data shown in Fig. 5. Curves (1) and (2) in Fig. 5 represent respectively the $n_s$ and $\mu$ values obtained in a Van der Pauw device irradiated to a $^1H^+$ dose slightly lower than that corresponding to D1 case. It is clearly apparent the remarkable increasing of both $n_s$ and $\mu$ in the temperature range of 200–300 °C. This annealing behavior can be explained assuming annihilation of acceptorlike compensation centers. The increase of both $n_s$ and $\mu$ results respectively of electron liberation and reduction of the concentration of charged scattering centers. Pons *et al.*[14] using deep level transient spectroscopy (DLTS) in GaAs irradiated with 1 MeV electrons reported a pronounced annealing stage beginning at the same temperature. These


[This article is copyrighted as indicated in the article. Reuse of AIP content is subject to the terms at: http://scitation.aip.org/termsconditions. Downloaded to ] IP: 200.130.19.173 On: Fri, 21 Mar 2014 18:03:40

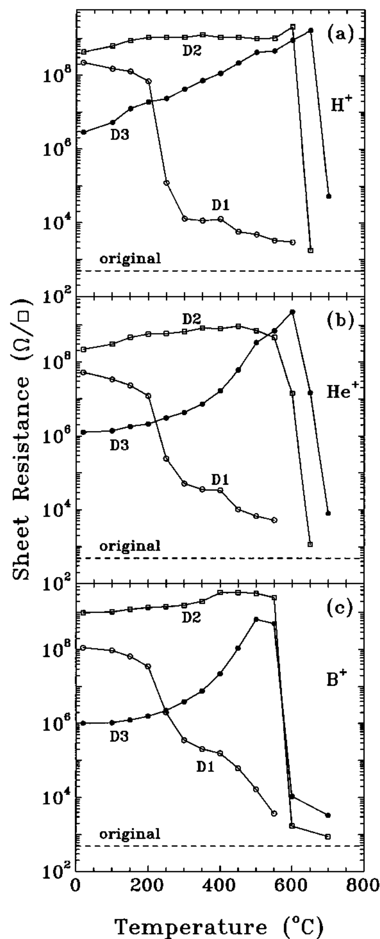


FIG. 4. The evolution of $R_s$ with the temperature of the post-irradiation annealing in samples irradiated with $H^+$ at 50 keV (a), $He^+$ at 80 keV (b), and $B^+$ at 150 keV (c). The ion doses were chosen to create the specific defect concentration levels D1, D2, and D3.

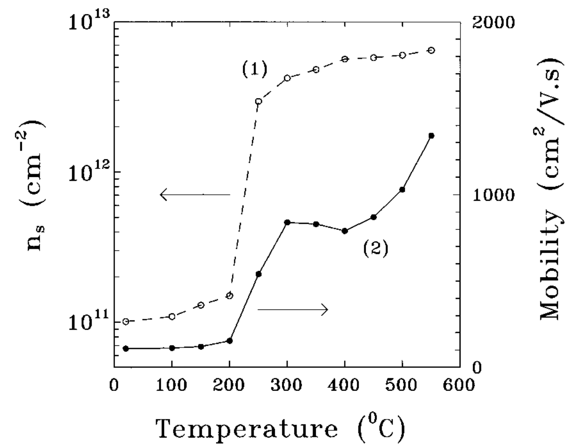


FIG. 5. Sheet carrier concentration $n_s$ [curve (1)] and effective Hall mobility $\mu$ [curve (2)] for a GaAs sample with an original $R_s$ of 300 Ω/□, subsequently irradiated with $H^+$ at 50 keV and dose $3\times10^{13}$ $cm^{-2}$ and isochronically annealed for 300 s at different temperatures. The original values of $n_s$ and $\mu$ are $1.36\times10^{13}$ $cm^{-2}$ and 1910 $cm^2$/V s, respectively.

authors interpreted the annealing mechanism as annihilation of simple intrinsic defects like vacancy-interstitial pairs or vacancy-antisite defect pairs. Considering that the $Ga_{As}$ antisite defects are double acceptors,[15] their annihilation would produce the observed enhancement of $n_s$. Probably the $Ga_{As}$ antisites recombine with $V_{Ga}$ vacancies at temperatures above 200 °C.

The height of the steps at 200–300 °C in the $R_s$ curves of Figs. 4(a)–4(c) decreases with the increasing of the ion mass. This seems to be related to the structure of the collision cascade. The collision cascades becomes denser with lesser amount of simple defects as the ion mass increases. Considering this annealing stage as associated to annihilation of simple intrinsic defects,[14] its contribution to the recovering of the conductivity is expected to decrease with the increasing of the ion mass.

The annealing stage beginning at 400 °C promotes enhancement of $\mu$ without increasing of $n_s$ [see curves (1) and (2) in Fig. 5]. Apparently, annealing of charged scattering centers without net carrier liberation is taking place. A most credible explanation for this phenomenon is the annihilation of defect pairs composed by an ionized donorlike defect and a negatively charged one.

The change of $\mu^{-1}$, which is proportional to variation of the concentration of charged scattering centers, was plotted versus the inverse of the temperature of the annealing (plot not shown). The $\mu$ values were obtained in Van der Pauw devices irradiated with $H^+$ (D1 case) and subsequently annealed at temperatures in the range from 400 to 500 °C. The straight line fitting to the data provided an activation energy of $0.51\pm0.02$ eV for the annealing of the charged scattering centers. This value agrees quite well with the migration energy of the As interstitial ($As_i$).[16] Presumably, the annealing at 400–500 °C arises from the recombination of $As_i^+$ (ionized donors) with negatively charged As vacancies ($V_{As}^-$).

Remarkable effects on the thermal stability of the isolation are introduced when the damage concentration level increases from D1 to D2 (see Fig. 4). For the samples irradiated to the D2 damage level, the interval of temperature for which the isolation persists extended to 550–600 °C. Above ≈550–600 °C there is a sharp decrease of $R_s$ toward its original value.

This annealing behavior closely correlates with those observed in previous works.[17,18] Wörner *et al.*[17] reported a sharp decrease of the $As_{Ga}^{4+}$ electron spin resonance signal in neutron irradiated GaAs, after annealing at temperatures above 500 °C. Martin *et al.*[18] demonstrated that temperatures in excess to 550 °C are required to anneal most of the damage in GaAs irradiated with $B^+$ to doses in the range of $10^{13}$–$10^{14}$ $cm^{-2}$.

Considering that the $As_{Ga}$ antisite annihilates via recombination with $V_{As}$ it is conceivable to assume that this annealing stage is assisted by thermally generated $V_{As}$. The possible sources for $V_{As}$ generation are: (i) the sample surface where significant As loss is expected to occur during capless post-irradiation annealing and, (ii) the dissolution of defect complexes.

In a separated experiment, samples capped with 50-nm-thick $Si_3N_4$ layer were irradiated with $H^+$ to a dose corre-


[This article is copyrighted as indicated in the article. Reuse of AIP content is subject to the terms at: http://scitation.aip.org/termsconditions. Downloaded to ] IP: 200.130.19.173 On: Fri, 21 Mar 2014 18:03:40

sponding to D2 damage concentration level and annealed together with capless ones. Besides the lower As loss from the capped surface, identical $R_s$ values were found in the capped and capless annealed samples. This result indicates that the contribution of the surface to the generation of $V_{As}$ is negligible. Very likely, $V_{As}$ and $V_{Ga}$ are generated predominantly from the thermal dissolution of complex lattice defects in samples submitted to high dose irradiation.

The essential process for electron liberation is the annihilation of acceptor defects, like the $Ga_{As}$ antisite. This annihilation reaction involves $V_{Ga}$ and is supposed to occur at a much lower temperature (at $\geqslant$200 °C). The simple defects predominate the irradiation damage. Consequently, in low dose irradiated samples, like D1 case, low temperature annealing is able to liberate most of the captured carriers. However, in samples irradiated to higher doses the residual trapping centers after annealing (200 °C$<$T$<$500 °C) consist of complex defects. Depending on the irradiation dose, their concentration may be high enough to keep the majority of the carriers captured. This would explain the lack of the annealing stage at 200 °C in the D2 and D3 curves of Figs. 4(a)–4(c). Annealing temperatures in excess to 500 °C are required to dissolve the defect complexes and generate the vacancies necessary for annihilation of the antisites.

For technological applications, the hopping conduction in samples irradiated to the highest doses (D3 case) has to be suppressed in order to attain high isolation between devices. An annealing performed at 400–550 °C is then required to obtain best isolation [see curves D3 in Figs. 4(a)–4(c)]. The hopping conduction ceases when the defect concentration in slab II, and very likely in slab I also, becomes sufficiently low such that the distance between the defects is large enough to preclude carrier hopping.

In spite of the higher damage concentration level in D3 case compared to D2 one, only a marginal improvement of $\approx$50 °C is observed in the thermal stability of $H^+$ and $He^+$ irradiated samples. In the case of $B^+$ irradiation no improvement is observed.

Based in the present study, we propose the concept that the isolation persists while the density of electron traps in the $n$-type GaAs layer exceeds that of the original carriers. In the case of an irradiation to a dose which creates a damage concentration comparable to that of carriers (D1 case), the annealing of even a small fraction of the electron trap concentration (at $\approx$200 °C) leads to carrier liberation and hence significant reduction of the $R_s$. In the case of D2, the trap concentration in the doped layer is about one order of magnitude higher than in the case of D1, as estimated by the dose ratios. This fact reflects in a higher thermal stability for the case of D2 compared to D1 one.

In the case of D3, the damage concentration is about one order of magnitude higher than in D2. However, the annealing kinetics at 550–650 °C is so high that the additional damage concentration produces, if any, a marginal improvement in the thermal stability of the isolation.

## IV. SUMMARY AND CONCLUSIONS

Initially, the evolution of the sheet resistance with the ion dose in $n$-type GaAs layers was analyzed in terms of the depth distribution of the irradiation damage. Subsequently, the thermal stability of the isolation after irradiations with ions of different mass, which form almost similar depth distribution of the damage was investigated. Three specific damage concentration levels labelled as D1, D2, and D3 were considered in the present study.

For a damage concentration which conducts to the onset of the isolation (D1), the stability is restricted to temperatures below 200 °C. We argue that this annealing stage results from reaction between simple isolated defects, the $Ga_{As}$ acceptors and $V_{Ga}$. At 400 °C, another annealing stage leads to the enhancement of the mobility without the increase of the carrier concentration. Very likely it proceeds via annihilation of charged scattering centers.

In the samples where a slightly hopping conduction is apparent (D2 case), the thermal stability of the isolation extends to temperatures of $\approx$550–600 °C. We argue that complex defects dissolution at temperatures above 550 °C generate the vacancies which react with the antisite defects, causing their annihilation.

Further increase of irradiation dose by another order of magnitude (D3 case) produces, if any, only a marginal improvement of the thermal stability.

In contrast with previous publications,[1,11] no significant mass effects influencing the thermal stability were found in the present work. The damage concentration is the main parameter influencing the thermal stability of the electrical isolation.

For application purposes, the dose corresponding to the damage level D2 leads to the highest isolation without demanding post-irradiation annealing. In addition, the thermal stability is comparable to those in samples irradiated to doses which lead to significant hopping conduction.

## ACKNOWLEDGMENTS

This work was partially supported by Financiadora de Estudos e Projetos (Finep), Fundação de Amparo a Pesquisa do Estado do Rio Grande do Sul (FAPERGS), Fundação de Amparo a Pesquisa do Estado de São Paulo (FAPESP), and Conselho Nacional de Pesquisas (CNPq).

[1] S. J. Pearton, Mater. Sci. Rep. **4**, 313 (1990).
[2] L. G. Salmon, J. Mat. Sci. Electron. **3**, 263 (1992).
[3] D. C. D'Avanzo, IEEE Trans. Electron Devices **ED-29**, 1051 (1982).
[4] J. P. de Souza and D. K. Sadana, Mater. Res. Soc. Symp. Proc. **240**, 887 (1992).
[5] Y. Kato, T. Shimada, Y. Shiraki, and K. F. Komatsubara, J. Appl. Phys. **45**, 1044 (1974).
[6] J. P. de Souza, I. Danilov, and H. Boudinov, Appl. Phys. Lett. **68**, 535 (1996).
[7] R. L. Van Tuyl, V. Kumar, D. C. D'Avanzo, T. W. Taylor, V. E. Peterson, D. P. Hornbuckle, R. A. Fisher, and D. B. Estreich, IEEE Trans. Electron Devices **ED-29**, 1031 (1982).
[8] F. Clauwaert, P. Van Daele, R. Baets, and P. Lagasse, J. Electrochem. Soc. **134**, 711 (1987).
[9] F. Ren, S. J. Pearton, W. S. Hobson, T. R. Fullowan, J. Lothian, and A. W. Yanof, Appl. Phys. Lett. **56**, 860 (1990).
[10] S. J. Pearton, C. R. Abernathy, J. W. Lee, F. Ren, and C. S. Wu, J. Vac. Sci. Technol. B **13**, 15 (1995).
[11] R. T. Blunt, in *Solid State Devices 1985*, edited by P. Balk and O. G. Folberth (Elsevier, the Netherlands, 1986), p. 133.
[12] L. J. Van der Pauw, Philips Res. Rep. **13**, 1 (1958).



[This article is copyrighted as indicated in the article. Reuse of AIP content is subject to the terms at: http://scitation.aip.org/termsconditions. Downloaded to ] IP: 200.130.19.173 On: Fri, 21 Mar 2014 18:03:40

[13] J. F. Ziegler, J. P. Biersack, and U. Littmark, *The Stopping and Range of Ions in Solids* (Pergamon, Oxford, 1985), Vol. 1.
[14] D. Pons, A. Mircea, and J. Bourgoin, J. Appl. Phys. **51**, 4150 (1980).
[15] W. J. Moore, R. L. Hawkins, and B. V. Shanabrook, Physica B & C **B146**, 65 (1987).
[16] J. C. Bourgoin, H. J. von Bardeleben, and D. Stievenard, J. Appl. Phys. **64**, R65 (1988).
[17] R. Wörner, U. Kaufman, and J. Schneider, Appl. Phys. Lett. **40**, 141 (1982).
[18] G. M. Martin, P. Secordel, and C. Venger, J. Appl. Phys. **53**, 8706 (1982).


[This article is copyrighted as indicated in the article. Reuse of AIP content is subject to the terms at: http://scitation.aip.org/termsconditions. Downloaded to ] IP: 200.130.19.173 On: Fri, 21 Mar 2014 18:03:40